OBSERVATIONS AND SPECTRAL ANALYSES OF SOLAR FLARES

M. D. DING

Department of Astronomy, Nanjing University, Nanjing 210093, China

E-mail: dmd@nju.edu.cn

ABSTRACT

We introduce the two-dimensional spectral observations of solar flares using the Solar Tower Telescope of Nanjing University, China. In particular, we introduce three typical events and the methods used to analyze the data. (1) The flare of November 11, 1998, which is a limb flare. We derive the temperature and density within the flaring loop using non-LTE calculations. The results show that the loop top may be hotter and denser than other parts of the loop, which may be a result of magnetic reconnection above the loop. (2) The flare of March 10, 2001, which is a white-light flare that shows an emission enhancement at the near infrared continuum. We propose a model of non-thermal electron beam heating plus backwarming to interpret the observations. (3) The flare of September 29, 2002, which shows unusual line asymmetries at one flare kernel. The line asymmetries are caused by an upward moving plasma that is accelerated and heated during the flare development.

Key words : line: profiles – Sun: flares – Sun: photosphere

I. INTRODUCTION

Solar flares are among the most energetic phenomena on the solar surface. The eruption of a flare involves a series of physical processes, such as the acceleration of energetic electrons, heating and dynamic evolution of the flare atmosphere, enhanced emission at various wavelengths etc. Flares are believed to originate from magnetic reconnection, during which a large amount of energy is released and a closed loop (flare loop) is formed. The loop is originally very hot and visible in soft X-ray; it then cools down through radiation and is finally visible in Hα. The energetics and dynamics of the Hα loop is of particular interest in understanding the energy transport processes in the flare atmosphere.

Using the imaging spectrograph installed at the Solar Tower of Nanjing University (Huang et al. 1995; Ding et al. 1999), we have performed spectral observations of solar flares since 1990's. We have obtained the two-dimensional (2D) spectra of two lines, Hα and Ca II λ8542, for more than 100 flares. The 2D spectral observations were performed using a scanning technique. Here, we introduce three typical flares that we have analyzed. In the following, we describe the spectral features, the methods to deduce the physical parameters, and some preliminary results for these three events.

II. THE FLARE OF NOVEMBER 11, 1998

(a) Observations

The flare (importance SF/C3.2) occurred at the northwest limb (N25 W86) on November 11, 1998. It began at 02:10 UT and ended at 02:18 UT, with a peak time at around 02:15 UT. During the flare eruption, we scanned over the flaring region to obtain a time series of 2D spectra in two lines, Hα and Ca II λ8542. A detailed description about the observations and data reduction can be seen in Ding et al. (1999).

Here, we select 12 scans for study which cover the whole evolution of the Hα flaring loop. The image drift during different scans is corrected by carefully co-aligning the images at the Hα wing, based on the sunspot features. We select three points in the loop: one at the loop top and the other two in the two feet of the loop, i.e., the footpoints. The loop geometry and the exact positions of the three points can be seen in Ding, Liu, & Chen (2002). The loop top point is of special interest because the Hα profile is found to be most broadened (Ding et al. 1999). We derive the temporal evolution of the temperature and density values at these points and make a comparison between them.

(b) The numerical method

We model the flaring loop as a vertical slab extending over the solar limb, as was done in Heinzel, Schmieder, & Mein (1992) and Gouttebroze, Heinzel, & Vial (1993). The slab has a finite width and two open boundaries that are irradiated by the radiation from the disk. Judging from the geometry of the loop, we take a slab width of 3,000 km. The temperature and mass density are assumed to be constant along the loop width (the line of sight). There is a background radiation field that is incident on the surfaces of the slab. The irradiation intensity is assumed to be half the mean intensity from the solar surface at all wavelengths. We do not consider a detailed transition region between the loop interior and the corona. Neglection of a detailed transition region has no great influence on the Hα and Ca II λ8542 lines, because they are formed in the main body of the loop.

The first step is to construct a large number of model slabs by varying the slab temperature (T) and the hy-

drogen density (n_H). For each model, we make non-LTE calculations to obtain the line profiles of Hα and Ca II λ8542 emergent from the slab surface. We then integrate the line intensities with respect to wavelength to get the integrated intensities as a two-dimensional function of T and n_H. The second step is to compare the observed and computed intensities of both lines, and to search for a solution of T and n_H which can best reproduce the observed values. This can be expressed as the following equations:

$$I^{\mathrm{o}}_{\mathrm{H}\alpha} = I^{\mathrm{c}}_{\mathrm{H}\alpha}(T, n_H), \qquad (1)$$

$$I^{\mathrm{o}}_{\lambda 8542} = I^{\mathrm{c}}_{\lambda 8542}(T, n_H), \qquad (2)$$

in which superscripts 'o' and 'c' refer to observed and computed values, respectively. The solution can be treated as the mean physical parameters in the loop.

The above technique is greatly simplified since there are several other factors that can influence the line intensity, such as the electron beam bombardment, the incident radiation, the micro-turbulent velocity. These parameters can vary temporally and spatially during the flare. We have tested carefully the effect of these factors. We find that assuming a non-thermal electron beam that is bombarding the plasma in the loop tends to increase the line intensities, as expected (see e.g., Fang, Hénoux, & Gan 1993). A direct consequence is to require a lower slab temperature. However, this effect is obvious only when $T < 10^4$ K, which is beyond the temperature range in the present case. Adopting a larger micro-turbulent velocity may broaden the line profile and also increase the integrated intensity. We find that it may lower the deduced temperature and/or the density. Comparatively, the effect of varying the incident radiation on the final results is small, because the slab is optically thick in most cases. In this work, we consider no electron beam bombardment, adopt a constant micro-turbulent velocity of 10 km s^{-1}, and an incident radiation field computed from a quiet-Sun model.

(c) Results

Table 1 gives the values of the temperature and the hydrogen number density at each time deduced using the method described above. We first notice that the values of T and n_H at the three selected points underwent a significant variation with the development of the flare. At the loop top, both the temperature and density peak at $\sim 02:15$ UT, roughly in coincidence with the soft X-ray maximum and the Hα maximum. At footpoint 1, a similar trend is found; at footpoint 2, however, the temperature and density seem to peak before the observation and decrease gradually at the time period studied here.

Another interesting phenomenon is that the loop top seems to be slightly hotter or condensed than the loop feet. From Table 1, it is seen that at the loop top, the deduced temperature varies in the range of 10,000–12,500 K, which is a typical value in post-flare loops.

However, the hydrogen number density reaches as high as $(1.0–3.5)\times10^{12}$ cm^{-3}. This higher density implies a shorter cooling time of the loop. In this case, we have estimated that the cooling time from soft X-ray to Hα loops is less than 1 min. This may explain the near simultaneity of the peaking time of the Hα emitting temperature and that of the soft X-ray flux. A higher density also implies that the flaring loop lies relatively lower.

The above results can be interpreted in terms of the current flare models. If magnetic reconnection occurs above the flaring loop, the outflow from the reconnection site impinges the closed loop and condenses the material there. The loop can also be heated through slow mode shocks as have been shown in numerical simulations (e.g., Chen et al. 1999). Another possibility to produce the higher mass density and velocity in the loop is chromospheric evaporation. This happens mainly in soft X-ray loops but has a direct relationship to the Hα loop because the cooling time of the loop is so short.

III. THE FLARE OF MARCH 10, 2001

(a) Observations

The flare (importance M6.7/1B) occurred at the position of N27 W42, in the active region NOAA 9368, on March 10, 2001. It started at 04:00 UT, peaked at 04:05 UT, and ended at 04:07 UT. Liu, Ding, & Fang (2001) and Ding et al. (2003) have studied the continuum features of this flare. They found that at the flare kernel, the continuum level near the infrared line Ca II λ8542 is enhanced by 3%–5% during the flare peak time. Considering the fact that there is a good time correlation between the continuum emission and the hard X-ray (or microwave radio) emission, the flare is thought to be a type I white-light flare, heated mainly by a non-thermal electron beam (Fang & Ding 1995). On the other hand, they also found that, at the very beginning of the flare (the early impulsive phase), the continuum seems to be decreased slightly by $\sim 1\%$. Although this slight dip is within the observational error, it nevertheless provides a candidate of "black" (or negative) flares that have been theoretically predicted to exist (Hénoux et al. 1990).

(b) The model and numerical computations

To explain the continuum features for this flare, we need first to check the energy transport and heating processes in the flare atmosphere. As stated above, the close relationship of the hard X-ray emission and the optical emission implies that the non-thermal electrons may be the main heating source. A non-thermal electron beam can not only provides a heating to the chromosphere, but also cause non-thermal ionization and excitation of hydrogen atoms, thus enhancing greatly the emission in chromospheric lines, such as the Hα line (Fang, Xu, & Ding 2003). However, the contin-

TABLE 1

TEMPERATURE AND HYDROGEN NUMBER DENSITY AT THE THREE POINTS WITHIN THE FLARE LOOP

time (UT)	footpoint 1		footpoint 2		loop top	
	T (K)	n_H (cm^{-3})	T (K)	n_H (cm^{-3})	T (K)	n_H (cm^{-3})
02:12:09	10250	1.39×10^{12}	11900	2.62×10^{12}	11060	1.39×10^{12}
02:12:33	10390	1.51×10^{12}	12280	2.55×10^{12}	10510	9.63×10^{11}
02:12:47	10150	1.38×10^{12}	11910	2.52×10^{12}	10410	1.17×10^{12}
02:13:04	10520	1.74×10^{12}	11690	2.32×10^{12}	11380	2.41×10^{12}
02:13:34	10890	2.19×10^{12}	11340	2.15×10^{12}	11830	2.86×10^{12}
02:13:53	11280	2.67×10^{12}	11680	2.15×10^{12}	11200	2.50×10^{12}
02:14:17	11250	2.81×10^{12}	11560	2.04×10^{12}	11800	3.29×10^{12}
02:14:38	11320	2.75×10^{12}	11080	1.78×10^{12}	12210	3.57×10^{12}
02:15:07	11230	2.69×10^{12}	11080	1.58×10^{12}	12030	3.29×10^{12}
02:15:29	11240	2.64×10^{12}	11110	1.65×10^{12}	12070	3.65×10^{12}
02:15:57	11220	2.55×10^{12}	10690	1.45×10^{12}	11870	2.54×10^{12}
02:16:28	10880	2.19×10^{12}	10660	1.07×10^{12}	11390	2.06×10^{12}

uum near the Ca II $\lambda 8542$ line is formed rather deeper, mostly in the photosphere. Electrons of deka-keV energy are hard to penetrate directly to the photosphere. The problem is how the photosphere gets heated. The most probable mechanism is the chromospheric radiative backwarming (Machado et al. 1989; Metcalf et al. 1990). In the present case, radiation from the chromosphere is greatly enhanced by the bombardment of the electron beam; the photosphere absorbs this radiation and the temperature is increased there.

To test the above point, We make numerical computations to show how the lower atmosphere can be radiatively heated through the effect of backwarming, in particular in the presence of a non-thermal electron beam. The method is similar to that proposed by Aboudarham & Hénoux (1987).

We first calculate the radiative cooling rates in the background atmosphere with and without a non-thermal electron beam introduced. We regard the latter case as the pre-flare status and the former case as the beginning of flare heating. As expected, the cooling rates in both cases are non-zero. In a stationary atmosphere (the preflare atmosphere), a positive cooling rate requires a non-radiative heating process while a negative cooling rate implies energy excess that should be carried away by some unknown means in order for energy balance to hold. In the present study, we need only to pay attention to the relative change of the cooling rates from the thermal to the non-thermal case. In particular, in the lower atmosphere (the temperature minimum region and below), the cooling rate is originally negative in the thermal case; however, it becomes more negative in the non-thermal case. This fact implies that

the presence of a non-thermal electron beam can cause a heating effect in the lower atmosphere through radiation, even the electrons cannot directly reach such a lower depth.

We choose the atmospheric model F1 (Machado et al. 1980) as the background (preflare) atmosphere. Then we introduce an electron beam that is supposed to bombard the atmosphere. The atmosphere is heated to some extent, characterized by a decrease of the radiative cooling rate as stated above. We assume that after an enough long time (~ 15–25 s), the atmosphere gets fully heated, and energy balance is reached again. Therefore, under the constraint of energy balance, we reconstruct an atmospheric model by modifying the temperature structure semi-empirically. Denote by H the energy deposition rate by the electron beam and Φ_{NT} and Φ_T the radiative cooling rates in the non-thermal and thermal cases, respectively. In principal, we require that

$$H = \Phi_{NT}(T + \Delta T) - \Phi_T(T). \qquad (3)$$

In fact, in the lower atmosphere, H is relatively small, which means that the decrease of the cooling rate in the non-thermal case relative to the thermal case should be compensated for by a temperature increase. In Table 2, we give the temperature increase, ΔT, at the layer ($m = 1$ g cm^{-2}) for a case of electron beam heating. As usual, we assume a power law distribution for the electron beam. We vary the energy flux, $\mathcal{F}_1$, of the beam but fix the low-energy cut-off, E_1, to be 20 keV and the spectral index, δ, to be 4.

From the table, we can find a significant temperature rise in the lower atmosphere in response to the back-

TABLE 2

TEMPERATURE INCREASE AT $m = 1$ G CM^{-2} AND CONTINUUM CONTRAST AT $\lambda = 8500$ Å

$\mathcal{F}_1$	ΔT	continuum contrast	
(ergs cm^{-2} s^{-1})	(K)	(case 1)	(case 2)
3×10^9	70.	−0.34%	2.67%
1×10^{10}	140.	−0.66%	7.47%
3×10^{10}	220.	−1.25%	9.72%
1×10^{11}	280.	−2.53%	10.03%

warming effect. We then calculate the continuum emission at $\lambda = 8500$ Å. For a better comparison with observations, we consider two cases: a background atmosphere with a precipitating electron beam and a heated atmosphere with an electron beam. These two cases can be roughly regarded as the early impulsive phase (the onset of electron heating) and the flare maximum phase, respectively. The calculated continuum contrast (relative change of the continuum compared to the pre-flare value) is also listed in Table 2.

It is interesting that in the first case, i.e., the pre-flare atmosphere bombarded by an electron beam, the continuum at $\lambda = 8500$ Å is decreased. This supports the previous conclusion by Hénoux et al. (1990) that "black" (or negative) flares may exist on the Sun. A further study shows that such a continuum dimming is caused by an absorption of an enhanced H$^-$ opacity that is produced by the non-thermal ionization effect of the electron beam. With flare development, the atmosphere gets heated through backwarming. We then move to the second case, in which the continuum rises above the preflare value. This corresponds to the origin of white-light flares.

We have also deduced the energy flux and the power index of the electron beam for this flare based on the hard X-ray emission observed by *Yohkoh*. We find that, during the impulsive phase ($\sim$ 04:03–04:04 UT), the power index varies in the range of 3–6. If we take a low-energy cut-off of 20 keV, the energy flux reaches a maximum of $\gtrsim 10^{11}$ ergs cm^{-2} s^{-1}. Judging from Table 2, such an electron beam seems to be strong enough to produce the continuum dip at the beginning and the continuum enhancement at the maximum phase as revealed by observations.

IV. THE FLARE OF SEPTEMBER 29, 2002

(a) Observations

The flare (importance M2.6/2N) occurred at a location of N12 E21 on September 29, 2002. It is a flare with a relatively short duration. It started from 06:32 UT, peaked at 06:39 UT, and ended at 06:41 UT. Our
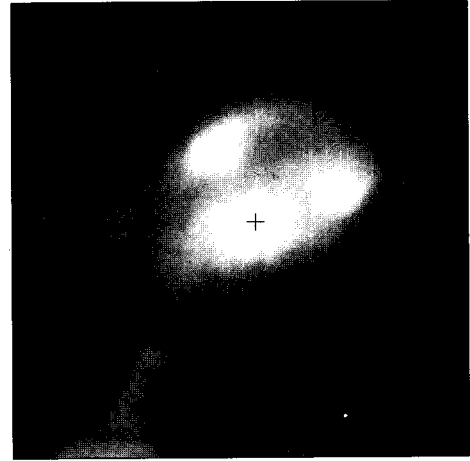

Fig. 1.— The flare image at the Hα line center at 06:35:58 UT on September 29, 2002. The field of view is $75'' \times 75''$. The cross sign refers to the position where the line profiles are plotted in Fig. 2.

spectral observations were done in the period of 06:35–06:49 UT. The seeing was fairly good during the observations.

(b) Characteristics of the spectral lines

Our 2D spectral data provide the spectral features varying in both space and time, therefore valuable for studying the dynamics of the flaring atmosphere. The flare of September 29, 2002 is a good example that shows the complexity of spectral features. Figure 1 shows the monochromatic image of this flare at the Hα line center. There are several bright patchs in the flaring region. The spatial connection of the flare ribbons are still under study. Here we make some preliminary analysis. We plot in Figure 2 the excess Hα and Ca II λ8542 line profiles at one kernel, shown as a cross in Figure 1, as a function of time. The excess profiles are defined as the flare profiles subtracted by the quiescent profile, which, in our case, is taken as the profile well after the flare. We can find an interesting variation of the
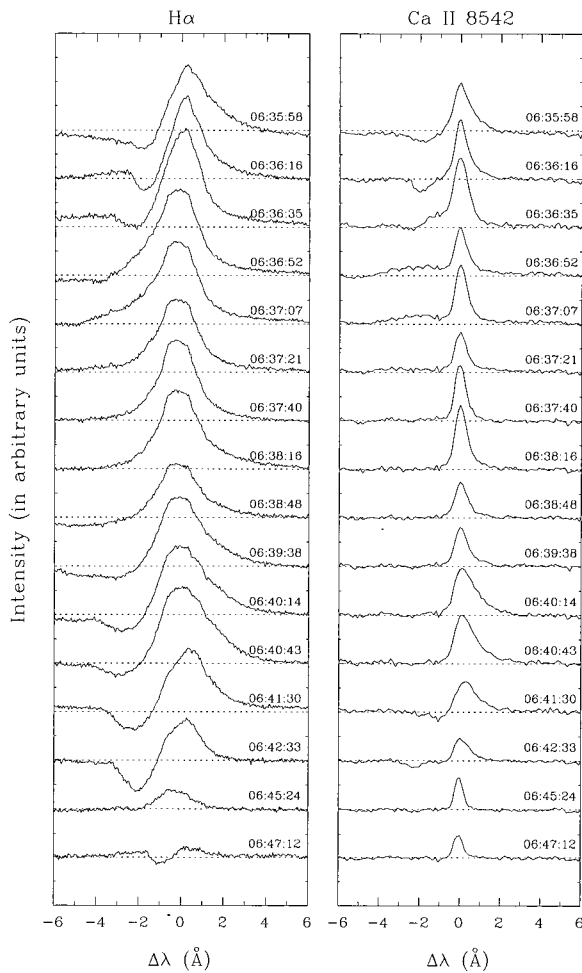
Fig. 2.— The Hα and Ca II λ8542 line profiles (with the quiescent profile subtracted) at one flare kernel as shown in Fig. 1.

the moving material is cooler or hotter than the radiation temperature, that is, whether it is absorptive or emissive to the radiation from below. Therefore, in this scenario, the blue asymmetry is interpreted as a red-wing absorption.

However, the present event seems to be different from the above model. The observed blue-wing absorption and emission is more likely produced by upward moving material. At first, the material is relatively cool so that it produces an absorption in the blue wing. With the flare development, the material is gradually heated and it produces an emission in the blue wing. After the maximum phase, it cools down and makes absorption again. Judging from the time history of the Doppler velocity, the upward moving material shows acceleration in the heating phase and deceleration after the flare maximum. The maximum velocity seems to exceed 100 km s^{-1}. On the other hand, the red asymmetry shown at the maximum phase can still be explained as due to the chromospheric condensation.

The observational features described above suggest that the moving material is most probably a flare-associated surge. The acceleration and the heating of the surge are closely related to the flare development. A detailed study of the dynamics of the flare and the surge will be made in a future work.

ACKNOWLEDGEMENTS

REFERENCES

Aboudarham, J., & Hénoux, J.-C. 1987, A&A, 174, 270

Chen, P. F., Fang, C., Ding, M. D., & Tang, Y. H. 1999, ApJ, 520, 853

Ding, M. D., & Fang, C. 1997, A&A, 318, L17

Ding, M. D., Fang, C., Yin, S. Y., & Chen, P. F. 1999, A&A, 348, L29

Ding, M. D., Liu, Y., & Chen, P. F. 2002, Solar Phys., 207, 125

Ding, M. D., Liu, Y., Yeh, C.-T., & Li, J. P. 2003, A&A, in press

Fang, C., & Ding, M. D. 1995, A&AS, 110, 99

Fang, C., Hénoux, J.-C., & Gan, W. Q. 1993, A&A, 274, 917

Fang, C., Xu, Z., & Ding, M. D. 2003, JKAS, 36, S55

Gouttebroze, P., Heinzel, P., & Vial, J. C. 1993, A&AS 99, 513

Heinzel, P., Schmieder, B., & Mein, P. 1992, Solar Phys., 139, 81

Hénoux, J.-C., Aboudarham, J., Brown, J. C., van den Oord, G. H. J., van Driel-Gesztelyi, L., & Gerlei, O. 1990, A&A, 233, 577

profiles. In an early time (the early impulsive phase), the line profiles show a blue-shifted absorption; shortly after this, the blue-shifted absorption turns to blue-shifted emission (blue asymmetry); then, at nearly the maximum phase, a red asymmetry appears, followed again by a blue-wing absorption. Such an evolution behavior appears in both lines, although it is clearer in Hα than in Ca II λ8542.

Since the Hα and Ca II λ8542 lines are optically thick in the flare atmosphere, one should be very cautious in explaining the spectral features or inferring the dynamics behavior of the atmosphere. Previous studies indicated that at the early impulsive phase, a blue asymmetry would appear; shortly afterwards, a red asymmetry sets in and lasts till the later phase. Ding & Fang (1997) proposed that both the blue asymmetry and red asymmetry may be caused by downflows (chromospheric condensation). The difference is only whether

Huang, Y. R., Fang, C., Ding, M. D., Gao, X. F., Zhu, Z. G., Yin, S. Y., Hu, J., & Xue, Y. Z. 1995, Solar Phys., 159, 127

Liu, Y., Ding, M. D., & Fang, C. 2001, ApJ, 563, L169

Machado, M. E., Avrett, E. H., Vernazza, J. E., & Noyes, R. W. 1980, ApJ, 242, 336

Machado, M. E., Emslie, A. G., & Avrett, E. H. 1989, Solar Phys., 124, 303

Metcalf, T. R., Canfield, R. C., & Saba, J. L. R. 1990, ApJ, 365, 391